

Anodic oxidation as a means to produce memristive films

*Original*

Anodic oxidation as a means to produce memristive films / Diamanti, Maria Vittoria; Pisoni, Riccardo; Cologni, Andrea; Brenna, Andrea; Corinto, Fernando; Pedferri, Maria Pia. - In: JOURNAL OF APPLIED BIOMATERIALS & FUNCTIONAL MATERIALS. - ISSN 2280-8000. - STAMPA. - 14:3(2016), pp. 290-295. [10.5301/jabfm.5000290]

*Availability:*

This version is available at: 11583/2657645 since: 2017-05-03T12:29:28Z

*Publisher:*

Wichtig Publishing Srl

*Published*

DOI:10.5301/jabfm.5000290

*Terms of use:*

This article is made available under terms and conditions as specified in the corresponding bibliographic description in the repository

*Publisher copyright*

(Article begins on next page)

# Anodic oxidation as a means to produce memristive films

Maria Vittoria Diamanti<sup>1</sup>, Riccardo Pisoni<sup>1</sup>, Andrea Cologni<sup>1</sup>, Andrea Brenna<sup>1</sup>, Fernando Corinto<sup>2</sup>, MariaPia Pedeferra<sup>1</sup>

<sup>1</sup>Giulio Natta Department of Chemistry, Materials and Chemical Engineering, Politecnico di Milano, Milan - Italy

<sup>2</sup>Department of Electronics and Telecommunications, Politecnico di Torino, Turin - Italy

## ABSTRACT

**Purpose:** In the past few years there has been growing interest in memristive devices. These devices rely on thin metal oxide films with a peculiar structure and composition, making precise control of oxide features vital. To this end, anodic oxidation allows a very large range of oxides to be formed on the surface of valve metals, whose thickness, structure and functional properties depend on the process parameters introduced. This work reports how memristive anodic oxides were obtained on titanium and other valve metals, such as niobium and tantalum.

**Methods:** Anodic oxidation was performed on valve metals by immersion in  $H_2SO_4$  or  $H_3PO_4$  electrolytes and application of voltages ranging from 10 to 90 V. The memristive behavior was evaluated by cyclic voltammetry.

**Results:** The behavior of differently grown oxides was compared to identify the best conditions to achieve good memristive performances. High voltages were identified as not suitable due to the excessive oxide thickness, while below 20 V the film was not thick and uniform enough to give a good response. Surface preparation also played a major role in the observation of memristive properties.

**Conclusions:** Optimal surface preparation and anodizing conditions were seen to give high memristive performances on both titanium and niobium oxides, while on tantalum oxides no reproducibility was achieved.

**Keywords:** Anodic oxidation, Memristor, Niobium, Spectrophotometry, Tantalum, Titanium dioxide

## Introduction

Information storage devices are dominated by silicon technology and nanotechnologies, which have led to circuit elements being shrunk to below 100 nm. Si-based flash memories represent the most diffuse nonvolatile memory (NVM) systems, owing to high data density and low fabrication costs. Still, they suffer from low endurance, low write speed, and high voltages required for write operations; moreover, downscaling is now reaching physical limits, as features size cannot keep shrinking at the current speed, posing a limit to memory density.

To overcome current NVM problems, several alternative memory concepts are being explored. Among these, NVMs based on resistance (switching) random access memory (RRAM) have attracted the most attention (1-3). The work presented here deals with a particularly interesting class of RRAM in which redox reactions and nano-ionic transport processes play the key role: memristive devices. Memristors

were first theorized in 1971 (4), but only in 2008 was a memristive characteristic actually observed in a metal/oxide/metal device built with Pt and  $TiO_2$  (5). The memristive behavior of  $TiO_2$  is based on the presence of oxygen vacancies moving forward and backward across the electronic barrier at the metal/oxide interface, generally through the formation of an oxygen vacancy filament, which results in changes to oxide resistance (6-9). The existence of such a filament has already been proved both experimentally by applying microscopy-based techniques, and through modeling (10-14).

This research study presents the technique of anodic oxidation as a means to produce metal oxides with added functionalities, specifically a memristive behavior, with a special focus on titanium, niobium and tantalum oxides (15). This technique can lead to the controlled production of oxide films on valve metals, and to the tuning of growth kinetics and oxide properties as a function of process parameters. Controlling electrochemical parameters (cell voltage, electrolyte composition, anodizing time) defines the oxide thickness, morphology, chemical and structural composition (15-17), which in turn is responsible for titanium surface properties such as corrosion resistance, insulation or biocompatibility (18, 19). Anodizing is a cheap, room-temperature alternative to physical and chemical fabrication methods typical of the electronics industry that are currently applied to memristor production. Furthermore, anodizing has already been demonstrated as suitable for producing memristive  $TiO_2$  films (11, 20).

Accepted: March 17, 2016

Published online: May 30, 2016

### Corresponding author:

Maria Vittoria Diamanti  
Politecnico di Milano  
Via Mancinelli 7  
20131 Milan, Italy  
mariavittoria.diamanti@polimi.it



## Materials and methods

Anodic oxidation was performed first on titanium specimens of grade 2 following ASTM classification: 30 × 20-mm samples were cut out of a 0.5-mm thick sheet. After a series of optimization tests on titanium, niobium and tantalum were also anodized under similar conditions: both Nb and Ta were purchased in 0.1-mm thick sheets from Goodfellow. Two electrolytes were considered: sulfuric acid (0.5 M) and phosphoric acid (0.5 M), with cell voltage ranging from 0 to 100 V. Particular attention was given to low voltage oxides (25 and 30 V). Before anodizing, the metal sheet was degreased with acetone. A surface preparation step also included either mechanical or chemical polishing, performed by abrasive papers down to 1200 grit, or with a mixture of HF and HNO<sub>3</sub>, 2.5% and 17.5% by weight, respectively. The specimen was then immersed in the electrolytic cell with an activated titanium net as a counter electrode, and a constant current density was applied. The anode-to-cathode potential difference increased gradually until the desired cell voltage was reached. Current density was 10 mA/cm<sup>2</sup>.

Tests were carried out at room temperature (approx. 25°C) with no cooling and no stirring: therefore, a slight heating of the electrolyte may have occurred at high voltages in sulfuric acid due to sparking phenomena (15). Given the low current density employed and large volume of electrolyte (0.5 L) this effect was considered negligible (in the order of room temperature fluctuations) since it becomes consistent only above 100 V in the presence of large current dissipations and large oxide crystallization, neither of which were observed in this case.

After anodic oxidation the reflectance spectrum of the anodized surface was measured in the visible range by means of a Konica Minolta CM-2600d portable reflectance spectrophotometer, operating in the range of 360 to 740 nm. Given the low thickness (30–200 nm range) of the oxides produced and their amorphous nature, interference of light with the oxide film grown on the metal surface caused the appearance of interference colors, whose reflectance spectra present a sinusoidal trend. Constructive and destructive interference occurring at different wavelengths creates peaks and valleys, respectively, whose position can be associated with the oxide thickness, as described in several studies (15, 16). To calculate oxide thickness from reflectance spectra, metal oxide refractive indexes are needed. The following values of refractive index at 550 nm were chosen:  $n_{Ti} = 2.2$ ,  $n_{Nb} = 2.3$ ,  $n_{Ta} = 2.1$  (21–26).

Once the oxide thickness was characterized, cyclic voltammetry was used to signal the possible achievement of a memristor. To meet this aim, the current-voltage response of the material was recorded under a cyclic voltage scan. The anodized titanium sheet was used as a working electrode by connecting the back of the titanium sample to the positive pole of the power supply, while a vertical rod with a 2-mm diameter copper tip was employed as a counter electrode. The rod tip was put in direct contact with the oxide layer: in this way, we obtained a metal-oxide-metal contact with the configuration copper-TiO<sub>2</sub>-titanium substrate, which allowed the electric properties of the oxide layer to be investigated. The cell voltage was ramped linearly versus time from 0 to  $V_f$

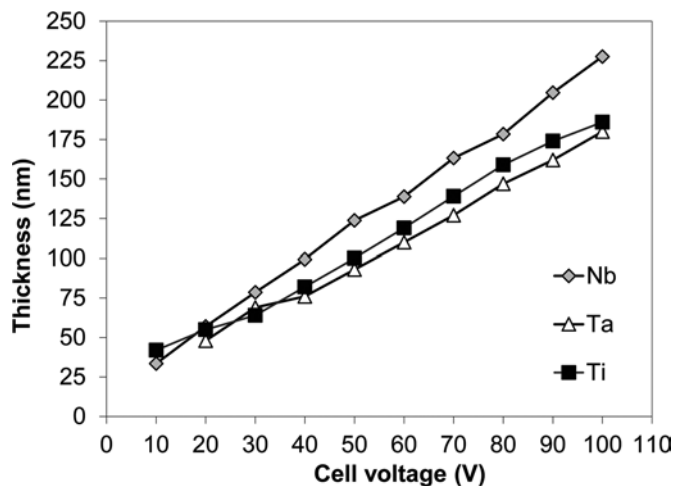


Fig. 1 - Thickness-voltage relationship of titanium, niobium and tantalum anodized in H<sub>2</sub>SO<sub>4</sub>.

(0.5 V <  $V_f$  < 1 V), then the scan was inverted until the specular negative potential  $-V_f$  was reached ( $-1\text{ V} < -V_f < -0.5\text{ V}$ ). Finally, the voltage was ramped back to the initial 0 V. Unless otherwise stated, the scan rate was set to 4 V/min.

## Results and discussion

As observed in previous works, a linear relation between oxide thickness and applied voltage emerges. Figure 1 shows, for the same electrolyte, the oxide thickness obtained by anodizing the 3 metals (Ti, Nb, Ta) calculated from reflectance spectra, plotted versus applied voltage. The anodizing ratio varies from 1.65 to 2 nm/V in both electrolytes (15, 27).

The growth of applied voltage in time, representing anodizing kinetics, is reported in Figure 2A for the 2 metals anodized in sulfuric acid electrolyte. The anodizing kinetics of titanium in sulfuric acid clearly slows down with time and with progressive oxide thickening. This is due to significant oxygen evolution taking place at the titanium surface as a parasitic reaction, which decreases process efficiency. Indeed, during anodizing it is possible to clearly detect oxygen bubbles forming at the metal surface (Fig. 2B). Oxygen evolution gets more evident above 70 V: this is due to the concomitant onset of oxide breakdown phenomena typical of anodic spark deposition, which heat up the electrolyte and reduce process efficiency. This was not observed when anodizing on niobium and tantalum in the same electrolyte: the process maintained the same speed until the maximum voltage, revealing a higher process efficiency with decreased dissipation. The importance of sparking phenomena and related heating in slowing down anodizing kinetics was clearly observed (Fig. 3). This hypothesis was further supported by the presence of crystalline oxide only on Ti, while Nb and Ta did not present any crystallization (27).

After anodizing, specimens were subjected to cyclic voltammetry analyses. Current-voltage (I-V) curves of memristors typically present a hysteretic loop, characterized by a high resistance state (low slope,  $R_{off}$ ) which switches to low resistance (high slope,  $R_{on}$ ) when a voltage threshold is

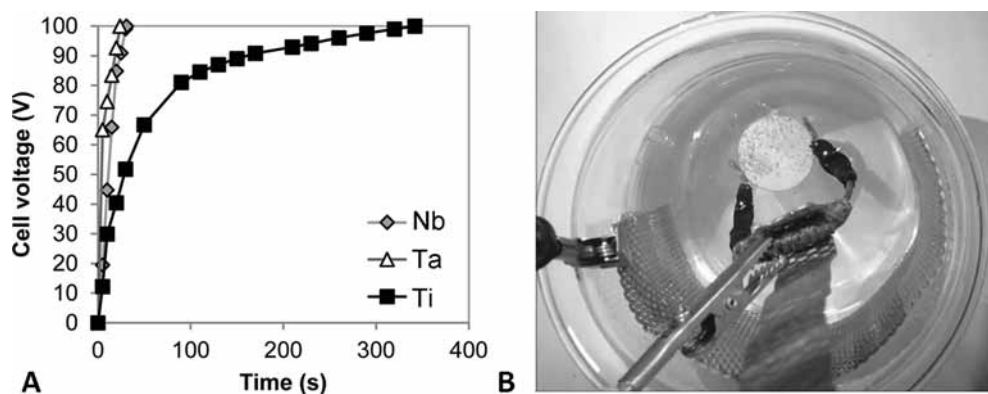


**Fig. 2 - (A)** Anodizing kinetics recorded during titanium anodizing and **(B)** oxygen evolution on titanium during anodizing, visible in the form of small bubbles on the surface.

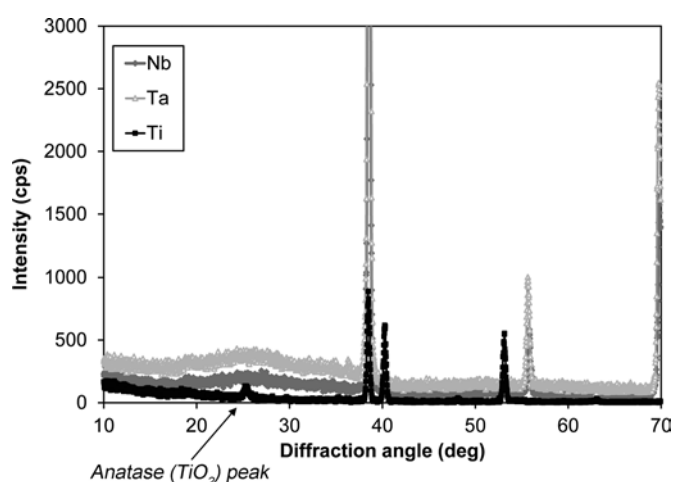


**Fig. 3 - X-ray diffraction spectra of titanium, niobium and tantalum anodized at 100 V.**

exceeded, and vice versa when a new voltage threshold occurs (Fig. 4). This pinched loop was observed on most of the anodic oxides tested in the positive and negative quadrants of the I-V diagram, although with different degrees of shape regularity, symmetry, and high-to-low resistance ratio ( $R_{\text{off}}/R_{\text{on}}$  ratio). These are the governing features in qualifying memristive switching as reliable. Therefore, anodizing parameters (voltage, electrolyte composition and concentration, metal substrate) were varied in order to understand the trends of memristive features with oxides of different thickness, composition and structure, and therefore to identify optimal anodizing conditions.

At first, the different oxide thicknesses produced by increasing cell voltages was considered a fundamental parameter for defining memristive performance: memristivity is supposed to depend inversely on oxide thickness (5, 28). In fact, what was observed was an increasing trend in loop opening (i.e.,  $R_{\text{off}}/R_{\text{on}}$  ratio) and symmetry with cell voltage until 30 V was reached, with a maximum loop opening at 25 V, above which the memristive response started to deteriorate (Fig. 5). In particular, loops appeared to be less open in the positive quadrant at increasing voltages. This was therefore associated with an exceedingly high oxide thickness, which made the oxide too insulating and hindered the

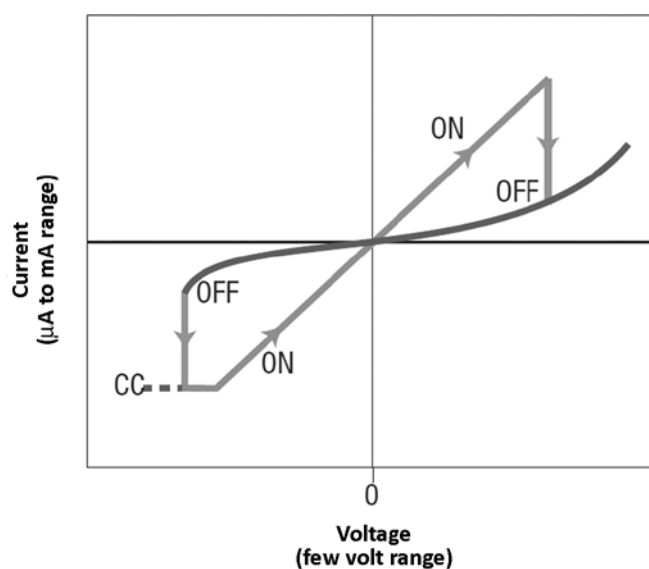


**Fig. 4 - Bipolar switching characteristics in a voltage sweeping experiment. The set operation takes place on 1 polarity of the voltage or current, and the reset operation requires the opposite polarity. (Reprinted from: Waser R, Aono M. Nanoionics-based resistive switching memories. Nature Mater. 2007; 6: 833-840 with permission from Nature Publishing Group)**

possible formation of through-thickness conductive channels, leading to a decay in memristive properties. On the other hand, at 90 V greater conductivity was noticed, which is related to the peculiar microstructure of oxides grown at high voltages: in these conditions the oxide is partially crystalline due to the onset of sparking phenomena, and to contain defects like porosities and cracks (15). Such features work together to modify its behavior, as already assessed in a previous work dedicated to the evaluation of anodic films as barriers against corrosion, in which their protectiveness was observed to decrease once sparking occurred (29).

Very thin anodic oxides did not behave as memristors, also owing to a possible island growth of the anodic oxide, which may still present conductive behavior below 10 V (approx. 40-nm thickness) due to parts of the metal surface that are still exposed to the environment. This peculiar growth behavior was observed in a previous work with conductive AFM

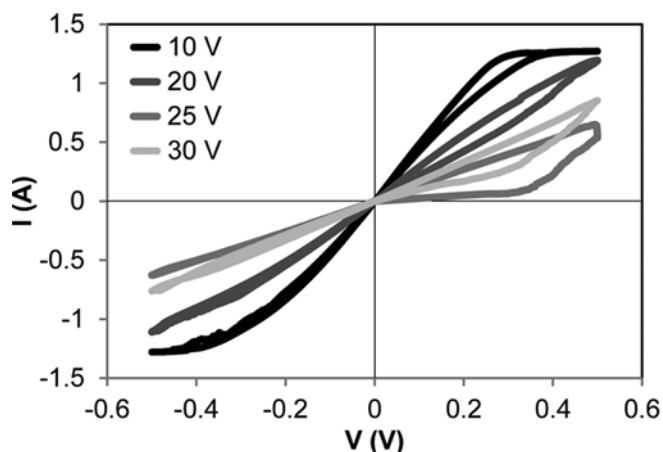


Fig. 5 - I-V curves obtained on oxides grown in sulfuric acid at different voltages.

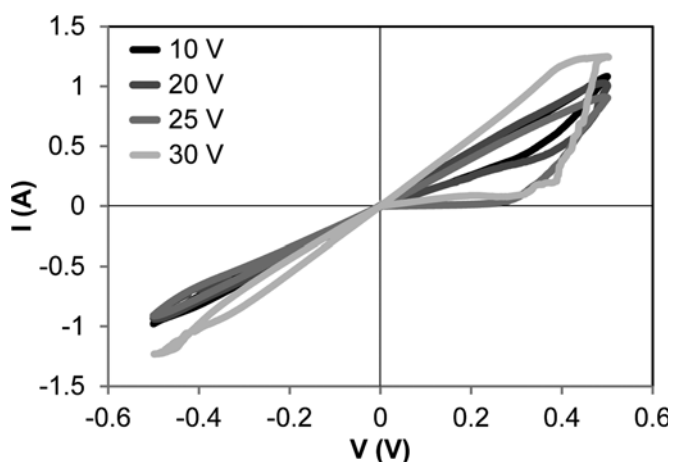
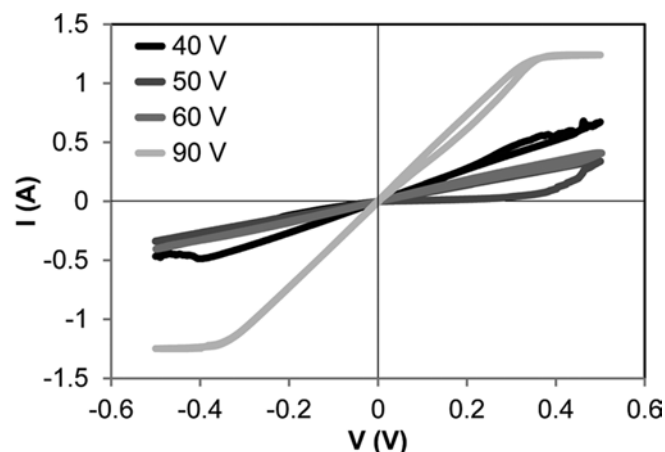


Fig. 6 - I-V curves obtained on oxides grown in phosphoric acid at different voltages.

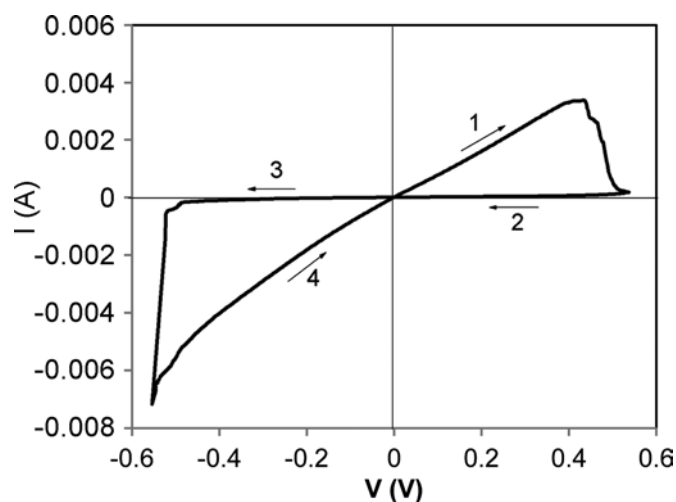


Fig. 7 - I-V curve obtained on mechanically polished titanium anodized in phosphoric acid at 30 V.

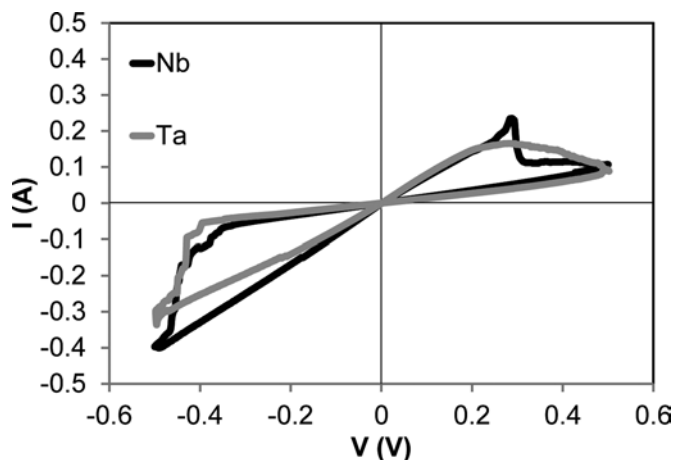
measurements (11). Consequently, the memristive response is shielded by the high conductivity of the metal.

Figure 6 reports cyclic voltammetry results performed on anodic oxides grown in phosphoric acid, with a concentration of 0.5 M as in the case of sulfuric acid. Only results related to low voltages (10-30 V) are shown, as they appear to be the most promising according to previously shown data. General results are far better than the corresponding samples anodized in  $\text{H}_2\text{SO}_4$ .

The sample anodized at 25 V was one of the best performing ones. Its  $R_{\text{off}}$  was evaluated to be approximately 17  $\Omega$ , while  $R_{\text{on}}$  was 0.5  $\Omega$ , which gives an off-on ratio higher than 30, representative of a good memristive element. As a comparison, oxides grown in  $\text{H}_2\text{SO}_4$  only produced a maximum off-on ratio of 6. Yet, a poor symmetry about the origin was obtained: this deviation may be ascribed to oxide defects, which may trap the motion of oxygen vacancies through the oxide. More interestingly, after repeating tests on mechanically polished samples in order to improve surface homogeneity, oxides produced in  $\text{H}_3\text{PO}_4$  exhibited a higher symmetry in the response (Fig. 7) together with a high  $R_{\text{off}}/R_{\text{on}}$  ratio. In

the cyclic voltammogram it is also possible to see the direction of cycles: at first a highly conductive state is present in the oxide, which switches and becomes more resistive at a voltage between 0.4 and 0.5 V, and a specular behavior was observed in the negative quadrant. This behavior is interpreted as the response of a defective  $\text{TiO}_2$  layer, whose resistivity increases as the oxygen vacancies drift towards one electrode under the electric field applied, modifying the charge carrier distribution in the oxide thickness and reducing its overall conductivity. When the polarity is inverted, oxygen vacancies migrate again in the opposite direction, redistributing across the oxide.

Based on the results described above, it was possible to define an optimized anodizing procedure, which consisted of subjecting the metal to mechanical polishing and anodic oxidation in  $\text{H}_3\text{PO}_4$  at voltages of either 25 or 30 V. The same procedure was then applied on niobium and tantalum: results are reported in Figure 8. Although  $\text{Ta}_2\text{O}_5$  oxide thickness was very close to that of titanium oxides grown in the same conditions, results were not as promising as in the case of memristive



**Fig. 8** - I-V curves obtained on mechanically polished niobium and tantalum anodized in phosphoric acid at 30 V.

TiO<sub>2</sub> films. This was due to the higher asymmetry and poor reproducibility of I-V curves, which varied consistently from one point of the oxide to another. On the contrary, Nb<sub>2</sub>O<sub>5</sub> films allowed performances similar to TiO<sub>2</sub> to be obtained, in terms of off-on ratio and reproducibility of the results.

In particular, anodized niobium exhibited interesting results, with performances similar to those of anodic TiO<sub>2</sub> combined with higher reproducibility of the experimental results.

Although a precise switching mechanism was not identified clearly, given the influence of a wide range of oxide features tested – thickness, composition, crystalline structure – it is generally accepted that voltage stresses applied during cyclic voltammetry drive the motion of oxygen ions through the oxide. Therefore, it is possible that a low resistance will be observed when the oxide has a homogeneous TiO<sub>2-x</sub> composition, since *x* is nearly at zero. Under an applied bias, oxygen ions moving towards the electrodes cause the accumulation of oxygen vacancies on one side of the oxide, reducing the compositional disorder in the oxide and therefore increasing its resistance.

## Conclusions

The experimental work here presented is aimed at identifying suitable anodizing conditions to achieve the formation of memristive oxides on valve metals, in particular titanium, niobium and tantalum. Oxide thickness plays a major role: neither too thin nor too thick anodic oxides need to be chosen to have a good memristive response, since the desirable oxide thickness ensuring complete surface coverage and avoiding the insulation provided by thicker layers is a few tens of nanometers. Concerning the metal substrate composition, only anodic Nb<sub>2</sub>O<sub>5</sub> and TiO<sub>2</sub> actually showed interesting switching properties, while several problems of reproducibility were experienced when analyzing Ta<sub>2</sub>O<sub>5</sub>.

## Disclosures

Financial support: This work was partly supported by the Alta Scuola Politecnica project MEM-BRAIN - MEMristor synapses for BRAIN computing.

Conflict of interest: The authors declare no conflict of interest.

## References

1. Waser R, Dittman R, Staikov G, Szot K. Redox-based resistive switching memories – Nanoionic mechanisms, prospects, and challenges. *Adv Mater.* 2009;21(25-26):2632-2663.
2. Gale E. TiO<sub>2</sub>-based memristors and ReRAM: materials, mechanisms and models (a review). *Semicond Sci Technol.* 2014; 29(10):104004.
3. Chua L. Resistance switching memories are memristors. *Appl Phys, A Mater Sci Process.* 2011;102(4):765-783.
4. Chua LO. Memristor - The Missing Circuit Element. *IEE Trans. Circuit Theory.* 1971;18(5):507-519.
5. Strukov DB, Snider GS, Stewart DR, Williams RS. The missing memristor found. *Nature.* 2008;453(7191):80-83.
6. Yang JJ, Pickett MD, Li X, Ohlberg DAA, Stewart DR, Williams RS. Memristive switching mechanism for metal/oxide/metal nanodevices. *Nat Nanotechnol.* 2008;3(7):429-433.
7. Waser R, Aono M. Nanoionics-based resistive switching memories. *Nat Mater.* 2007;6(11):833-840.
8. Choi BJ, Jeong DS, Kim SK, et al. Resistive switching mechanism of TiO<sub>2</sub> thin films grown by atomic-layer deposition. *J Appl Phys.* 2005;98(3):033715.
9. Larentis S, Cagli C, Nardi F, Ielmini D. Filament Diffusion Model for Simulating Reset and Retention Processes in RRAM. *Microelectron Eng.* 2011;88(7):1119-1123.
10. Kwon D-H, Kim KM, Jang JH, et al. Atomic structure of conducting nanofilaments in TiO<sub>2</sub> resistive switching memory. *Nat Nanotechnol.* 2010;5(2):148-153.
11. Diamanti MV, Souier T, Stefancich M, Chiesa M, Pedferri MP. Probing anodic oxidation kinetics and nanoscale heterogeneity within TiO<sub>2</sub> films by Conductive Atomic Force Microscopy and combined techniques. *Electrochim Acta.* 2014;129:203-210.
12. Lanza M, Bersuker G, Porti M, Miranda E, Nafria M, Aymerich X. Resistive switching in hafnium dioxide layers: local phenomenon at grain boundaries. *Appl Phys Lett.* 2012;101(19):193502.
13. Brivio S, Tallarida G, Cianci E, Spiga S. Formation and disruption of conductive filaments in a HfO<sub>2</sub>/TiN structure. *Nanotechnology.* 2014;25(38):385705.
14. Jo SH, Chang T, Ebong I, Bhadviya BB, Mazumder P, Lu W. Nanoscale memristor device as synapse in neuromorphic systems. *Nano Lett.* 2010;10(4):1297-1301.
15. Diamanti MV, Ormellese M, Pedferri MP. Application-wise nanostructuring of anodic films on titanium: a review. *J. Exp. Nanosci.* 2015;10(17):1285-1308.
16. Sul YT, Johansson CB, Jeong Y, Albrektsson T. The electrochemical oxide growth behaviour on titanium in acid and alkaline electrolytes. *Med Eng Phys.* 2001;23(5):329-346.
17. Vanhumbecq JF, Proost J. Current understanding of Ti anodization: functional, morphological, chemical and mechanical aspects. *Corros. Rev.* 2009;27(3):117-194.
18. Liu Z, Liu X, Donatus U, Thompson GE, Skeldon P. Corrosion behaviour of the anodic oxide film on commercially pure titanium in NaCl environment. *Int J Electrochem Sci.* 2014;9: 3558-3573.
19. Della Valle C, Rondelli G, Cigada A, Bianchi AE, Chiesa R. A novel silicon-based electrochemical treatment to improve osteointegration of titanium implants. *J Appl Biomater Funct Mater.* 2013;11(2):106-116.
20. Miller K, Nalwa KS, Bergerud A, Neihart NM, Chaudhary S. Memristive behavior in thin anodic titania. *IEEE Electron Device Lett.* 2010;31(7):737-739.
21. Coşkun ÖD, Demirel S. The optical and structural properties of amorphous Nb<sub>2</sub>O<sub>5</sub> thin films prepared by RF magnetron sputtering. *Appl Surf Sci.* 2013;277:35-39.
22. Arsova I, Arsov L, Hebestreit N, Anders A, Plieth W. Electrochemical formation of anodic oxide films on Nb surfaces: ellipsometric

- and Raman spectroscopic studies. *J Solid State Electrochem.* 2007;11(2):209-214.
23. Özer N, Rubin MD, Lampert CM. Optical and electrochemical characteristics of niobium oxide films prepared by sol-gel process and magnetron sputtering A comparison. *Sol Energy Mater Sol Cells.* 1996;40(4):285-296.
  24. Knorr K, Leslie JD. Ellipsometric measurements of the plasma oxidation of Nb and Ta and their interpretation. *J Electrochem Soc.* 1974;121(6):805-808.
  25. Leslie JD, Knorr K. Ellipsometric study of the plasma oxidation of tantalum. *J Electrochem Soc.* 1974;121(2):263-267.
  26. Van Gils S, Mast P, Stijns E, Terryn H. Color properties of barrier anodic oxide film on aluminium and titanium studied with total reflectance and spectroscopic ellipsometry. *Surf Coat Tech.* 2004;185(2-3):303-310.
  27. Diamanti MV, Garbagnoli P, Del Curto B, Pedferri MP. On the growth of thin anodic oxides showing interference colors on valve metals. *Current Nanosci.* 2015;11(3):307-316.
  28. Hu Y, Perello D, Yun M, Kwon DH, Kim M. Variation of switching mechanism in TiO<sub>2</sub> thin film resistive random access memory with Ag and graphene electrodes. *Microelectron Eng.* 2013;104:42-47.
  29. Diamanti MV, Bolzoni F, Ormellese M, Pérez-Rosales EA, Pedferri MP. Characterisation of titanium oxide films by potentiodynamic polarisation and electrochemical impedance spectroscopy. *Corros. Eng. Sci. Technol.* 2010;45(6):428-434.